

## Memory effect in the deposition of C<sub>20</sub> fullerenes on a diamond surface

A. J. Du,<sup>1</sup> Z. Y. Pan,<sup>1,2,\*</sup> Y. K. Ho,<sup>1</sup> Z. Huang,<sup>1</sup> and Z. X. Zhang<sup>1</sup>

<sup>1</sup>State Key Laboratory for Material Modification by Laser, Ion and Electron Beams, Institute of Modern Physics, Fudan University, Shanghai 200433, China

<sup>2</sup>Ion Beam Laboratory, Shanghai Institute of Microsystem and Information Technology, Chinese Academy of Science, Shanghai 20050, China

(Received 10 September 2001; revised manuscript received 27 March 2002; published 9 July 2002)

In this paper, the deposition of C<sub>20</sub> fullerenes on a diamond (001)-(2×1) surface and the fabrication of C<sub>20</sub> thin film at 100 K were investigated by a molecular dynamics (MD) simulation using the many-body Brenner bond order potential. First, we found that the collision dynamic of a single C<sub>20</sub> fullerene on a diamond surface was strongly dependent on its impact energy. Within the energy range 10–45 eV, the C<sub>20</sub> fullerene chemisorbed on the surface retained its free cage structure. This is consistent with the experimental observation, where it was called the memory effect in “C<sub>20</sub>-type” films [P. Melion *et al.*, *Int. J. Mod. B* **9**, 339 (1995); P. Milani *et al.*, *Cluster Beam Synthesis of Nanostructured Materials* (Springer, Berlin, 1999)]. Next, more than one hundred C<sub>20</sub> (10–25 eV) were deposited one after the other onto the surface. The initial growth stage of C<sub>20</sub> thin film was observed to be in the three-dimensional island mode. The randomly deposited C<sub>20</sub> fullerenes stacked on diamond surface and acted as building blocks forming a polymerlike structure. The assembled film was also highly porous due to cluster-cluster interaction. The bond angle distribution and the neighbor-atom-number distribution of the film presented a well-defined local order, which is of *sp*<sup>3</sup> hybridization character, the same as that of a free C<sub>20</sub> cage. These simulation results are again in good agreement with the experimental observation. Finally, the deposited C<sub>20</sub> film showed high stability even when the temperature was raised up to 1500 K.

DOI: 10.1103/PhysRevB.66.035405

PACS number(s): 61.43.Bn, 79.20.Rf, 61.46.+w

### I. INTRODUCTION

In recent years the low-energy cluster beam deposition technique (LECBD) has been becoming one of the promising methods to produce cluster-assembled films with hitherto unknown nanostructured morphologies and properties.<sup>1,2</sup> With the discovery of fullerenes,<sup>3</sup> fullerene-assembled materials, such as doped van der Waals bonded C<sub>60</sub> solids<sup>4</sup> and C<sub>28</sub> covalent bonded fullerenes,<sup>5</sup> received much attention due to their unique cage-like structure and unusual properties, especially, the superconductivity.<sup>6</sup>

Among them, the smallest fullerene C<sub>20</sub> is of particular interests because of the extreme curvature and reactivity. It has been recently synthesized in a gas phase by Horst Prinzbach *et al.*<sup>7</sup> and further confirmed theoretically by Mineo Satio *et al.*<sup>8</sup> It is only composed of pentagons. Each carbon atom in a C<sub>20</sub> cage is bonded to three others with a bond angle of 108°, which is close to the tetrahedral bond angle. There have been many theoretical studies on the vibrational and electronic properties of the C<sub>20</sub> cluster.<sup>9,10</sup> First principle studies of the condensed phases of C<sub>20</sub> cages suggested they might be possible superconductor with high transition temperature (*T<sub>c</sub>*).<sup>11</sup> Experimentally, “C<sub>20</sub>-type” film was synthesized by deposition of low-energy carbon clusters with a size distribution centered around C<sub>20</sub>-C<sub>32</sub>.<sup>12</sup> Raman spectra measured with the assembled film revealed the characteristics of *sp*<sup>3</sup> hybridization as that predicted for the C<sub>20</sub> fullerene. It is known that the growth process of C<sub>20</sub> film is difficult to observe experimentally. Furthermore, the issues of growth and chemical bonding of disordered C<sub>20</sub> solids, which involve cluster-cluster interactions, cluster-surface

interactions, and their competition, have not yet been addressed.

In this paper, the influence of impact energy on the collision dynamics of single C<sub>20</sub> interacting with substrate was first investigated by molecular dynamics simulations. Then the fabrication of C<sub>20</sub> fullerene-assembled film within an optimum energy range and the structure characteristics of “C<sub>20</sub>-type” films were studied in detail. The focus of our investigation was on the correlation between the structure of C<sub>20</sub> assembled film and that of a free C<sub>20</sub> cage.

### II. COMPUTATIONAL MODEL

In order to describe the interaction between C<sub>20</sub> and diamond surface, we employed the semiempirical many-body Brenner potential,<sup>13</sup> which was developed from Tersoff potential<sup>14</sup> with bond order function correction. The binding energy for this hydrocarbon potential is given as a sum over bonds by

$$E_b = \frac{1}{2} \sum_i \sum_{j \neq i} [V_R(r_{ij}) - \bar{B}_{ij} V_A(r_{ij})].$$

In the equation above, *E<sub>b</sub>* is the binding energy for the system and *V<sub>R</sub>*(*r<sub>ij</sub>*) and *V<sub>A</sub>*(*r<sub>ij</sub>*) are the repulsive and attractive potentials between atom *i* and atom *j*.  $\bar{B}_{ij}$  is the bond order function which is used to correct for an inherent overbinding of radicals and includes nonlocal effects. Although this potential was originally derived for simulation of diamond film synthesis through chemical vapor deposition (CVD), it has also been successfully applied to a wide range of other fields such as properties of fullerene,<sup>15</sup> fullerene and

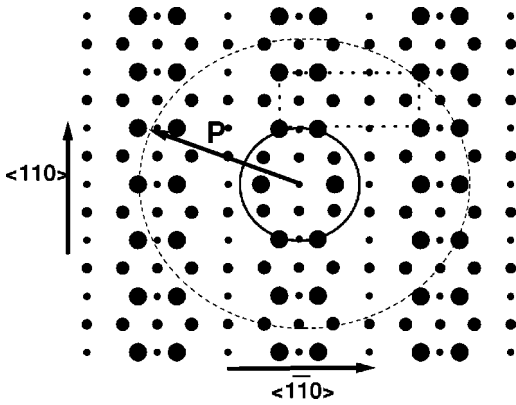


FIG. 1. Top view of a diamond (001)-(2 $\times$ 1) surface. The dotted rectangle is the area, where the impact position of single C<sub>20</sub> was selected. The dashed line circle represents the impact area of cage II where it interacts with cage I (solid line circle).

nanotube tip reaction with semiconductor surface,<sup>16–18</sup> etc. Compared to the sophisticated quantum mechanical approach, it is surely less accurate and cannot be used to calculate the electronic structure. However, our MD simulation based on this potential could deal with a larger size system with a few thousand atoms even on a personal computer and obtain the dynamical properties simultaneously.

Before processing the impact simulation, the geometric structure of C<sub>20</sub> was calculated by means of energy minimization method. The C<sub>20</sub> cage is composed of 12 pentagons and each atom on the vertices has a dangling bond. The binding energy of C<sub>20</sub> fullerene was calculated to be 6.36 eV/atom which was in good agreement with Ref. 19. The computed bond length was uniformly distributed in the interval from 0.144 to 0.153 nm, which is consistent with the *ab initio* method.<sup>20</sup> At the same time, the structure of two isomers, the C<sub>20</sub> bowl and ring, were also studied for comparison. The calculated binding energies of ring and bowl relative to cage were 4.92 and 3.45 eV/cluster higher, respectively. In the present calculation, the cage is the most stable structure, which agrees well with that of the LDA, but contradicts the result of the Quantum Monte Carlo approach.<sup>21</sup> However, within the energy range of the present investigation this effect has minor influence on the collision dynamics, which is strongly dependent on the initial orientation and incident energy of C<sub>20</sub> molecule.<sup>22</sup>

The diamond substrate was composed of eight layers with 324 atoms per layer. The bottom two layers were held fixed and the motion of atoms in the top two layers was determined by the force produced by the Brenner potential. The velocity scaling method of Nose-Hover thermostat<sup>23,24</sup> was applied to the middle four layers in order to maintain constant substrate temperature at 100 K. Periodic boundary conditions were employed in the two directions parallel to the surface.

Before starting the dynamics of the cluster-surface interaction, the C<sub>20</sub> cage was rotated randomly around its center-of-mass (c.m.) and positioned randomly in the *x-y* plane (Fig. 1). The *z* coordinate of C<sub>20</sub> was set at a distance sufficiently far away, where the interactions between the cage and the topmost atom of the substrate were negligible. The cage

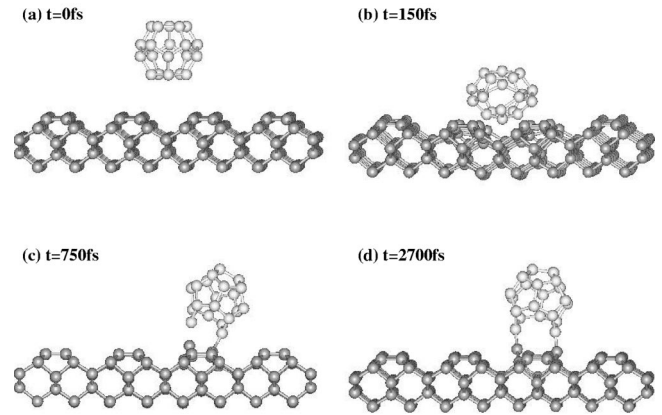


FIG. 2. Snapshots of atomic positions for a C<sub>20</sub> cage impacting on a diamond (001)-(2 $\times$ 1) surface. The impacting site was chosen in the middle of a trough and the incident energy was 25 eV.

was then projected normally onto the diamond surface. The trajectories of atoms in the simulation system were determined by integrating the equations of motion according to the Verlet algorithm.<sup>25</sup> The time step was selected to be 0.5 fs during the simulation. The C<sub>20</sub> cages impinged on the diamond surface one after the other. The time interval between successive impact was selected to be around 3.5 ps. During the simulation, the configuration energy was checked so that the next C<sub>20</sub> impact occurred after a full relaxation of the previous one.

### III. RESULTS AND DISCUSSION

#### A. Deposition of single C<sub>20</sub> fullerene on diamond surface

First, we provided the details about the impact of single C<sub>20</sub> fullerene on diamond (001)-(2 $\times$ 1) surface. The impinging position was randomly chosen from the dotted rectangular area in Fig. 1, which mapped the whole diamond surface. The incident energy ( $E_{in}$ ) was varied from 5 to 45 eV per cluster. The energy dependence of collision dynamics was examined. It was found that when the incident energy was lower than 8 eV, more than 80% of the incident C<sub>20</sub> cages were reflected off the surface without breaking up. Above 50 eV, fragmentation both in the cage and on the surface was observed. Between 10 and 45 eV, atoms in the normally incident C<sub>20</sub> fullerene could move collectively in a lateral direction. Finally, the C<sub>20</sub> cage was adsorbed either on a dimer or in a trough site of the dimerized surface, which are energy favored configurations.<sup>26</sup> Figure 2 shows snapshots of atomic positions for single C<sub>20</sub> impacting on diamond (001)-(2 $\times$ 1) surface at the incident energy of 25 eV. The impacting position was chosen in the middle of a trough. After arriving on the surface, the incident C<sub>20</sub> cage was first flattened due to the close cluster-surface interaction and one bond in C<sub>20</sub> was then broken. Then cluster atoms moved collectively in the transverse direction. Meanwhile one dimer bond on the diamond surface was also opened, with which the C<sub>20</sub> fullerene finally formed two bonds. The c.m. of the bonded C<sub>20</sub> fullerene moved a distance of 0.182 nm in the *x-y* plane. The binding energy was calculated to be 13.14 eV (6.57 eV/

bond). The bonded  $C_{20}$  cage had a structure similar to that of a free  $C_{20}$  cage (see Fig. 2). Each carbon atom in the cage had three neighbors. In addition, the bond length distribution of the bonded  $C_{20}$  fullerene was uniformly in the interval 0.142–0.155 nm, close to the value (0.144–0.153 nm) of a free  $C_{20}$  cage.<sup>22</sup> This illustrates that the bonded  $C_{20}$  cage almost retains its original cluster structure when the incident energy is within the range (10–45 eV), which is in agreement with the memory effect observed in LECBD experiment.<sup>12</sup>

It might be interesting to study whether the rotational energy (RE), which was supposed to be given in the condition of thermal equilibrium, will affect the growth dynamics. A new simulation model was thus established, which was similar to the former one except a rotational energy of  $C_{20}$  was added initially. Rotations of the cage were treated classically. The rotational energy was chosen as 0.001 eV corresponding to rotational temperature 20 K, because cluster beams produced via supersonic expansion were known to exhibit significant rotational cooling.<sup>27,28</sup> The adsorption probability (AP) was then calculated by adding the initial rotational velocities of each atom in the  $C_{20}$  molecule to their translational velocities. The statistics were accumulated over at least 100 events for each translational energy. At the incident translational energies 10, 15, and 20 eV, the calculated AP with additional rotational energy were 58.5, 62.9, and 67.2 %, respectively, close to the values of 58.0, 64.0, and 68.0 % without RE. Even at high rotational temperature of 3600 K, The calculated adsorption probabilities were only slightly changed to 61.3% for  $E_{in}=10$  eV and 70.5% for  $E_{in}=20$  eV, respectively. In addition, we found that within above energy range all the chemisorbed  $C_{20}$  fullerenes still preserved their free cluster structure. It indicates that in the present simulation, the initial rotation has minor effect on the collision dynamics of  $C_{20}$ . It can be understood from the spherelike geometry of  $C_{20}$ . In addition, in the present simulation of LECBD, the value of RE is much lower comparing with that of the incident translational energy ( $>10$  eV). This character is quite different from that of the trapping of ethane on Si, where the translational energy is much lower.<sup>29</sup> So in the following simulation of film fabrication, the rotational energy of  $C_{20}$  was neglected for the sake of simplicity.

### B. Deposition of the second $C_{20}$ fullerene near a chemisorbed one

In order to study the competition between the cluster-surface interaction and cluster-cluster interaction, a surface was designed with one  $C_{20}$  cage (cage I) already chemisorbed on a surface dimer (surface A), then a second  $C_{20}$  cage (cage II) with random orientation was dropped on it. The incident energy of cage II ranged from 10 to 25 eV. The lateral distance between the center-of-mass (c.m.) of two cages was defined as the impact parameter  $p$  if we consider the surface A as a target and cage II as a projectile (see the dashed circle in Fig. 1). The value of  $p$  was limited to be less than 0.6 nm, beyond which the collision dynamics of cage II is assumed to be unaffected by cage I. Figure 3 exhibits snapshots of atomic positions for cage II impacting on sur-

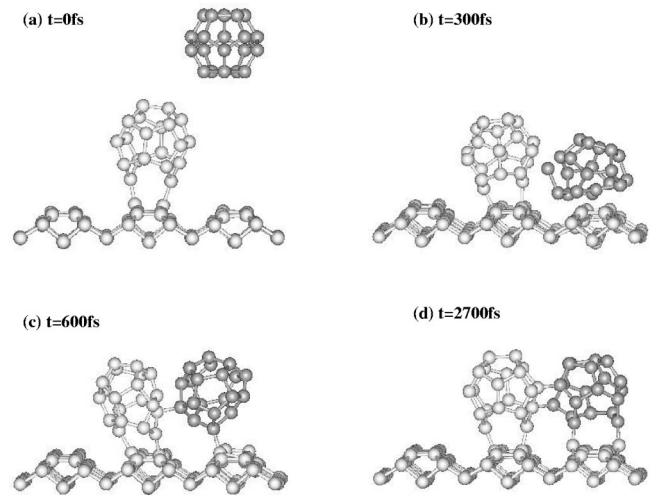


FIG. 3. Snapshots of atomic positions for cage II impacting on surface A [diamond (001) surface with a chemisorbed  $C_{20}$  fullerene]. The incident energy was 18 eV and the impact parameter was 0.5 nm.

face A (see Fig. 1). The incident energy was 18 eV and the value of  $p$  was 0.5 nm. After impact, cage II was first deformed due to the close interaction with cage I and the surface. Finally, a juxtaposition configuration of two  $C_{20}$  cages on the surface was formed. By varying the value of  $p$ , three possible chemisorption configurations (A, B, and C) were observed and shown in Fig. 4. Based on statistics accumulated over 100 events, the relative ratios corresponding to configurations A, B, and C was calculated as a function of  $p$ , and presented in Fig. 5. It was shown when  $p$  was less than 0.2 nm, the cluster-cluster interaction dominates the process and configuration A had the highest probability. Beyond 0.6 nm, the cluster-surface interaction takes the leading role and C is the most probable configuration. Within 0.25–0.6 nm, both cluster-cluster and cluster-surface interactions affect the collision dynamics causing the probabilities of configurations A, B, and C to be close to each other. For all these possible configurations (see Fig. 4), we observed that both adsorbed  $C_{20}$  cages retained the structure of the free  $C_{20}$  cage. The juxtaposition between  $C_{20}$  cages would dominate the structure of the  $C_{20}$  film, especially when the coverage is high. Judging from these configurations (especially configuration A), we expect the film assembled by deposition of  $C_{20}$  cages would be porous. Furthermore, the adsorption probability of  $C_{20}$  would be higher than that of  $C_{28}$  because of its dangling bonds and high reactivity.<sup>30</sup>

### C. Assembling of $C_{20}$ thin film

To study the fabrication of  $C_{20}$  assembled film, more  $C_{20}$  cages were deposited on the diamond (001)-(2×1) surface. The incident energies were uniformly distributed between 10 and 25 eV, which was close to the energy range (10–20 eV) in LECBD experiments.<sup>12</sup> We first found that the film grew in a typical three-dimensional island mode. The chemisorbed  $C_{20}$  cages randomly stacked and the second layer began to grow before the first layer was well covered. In our simula-

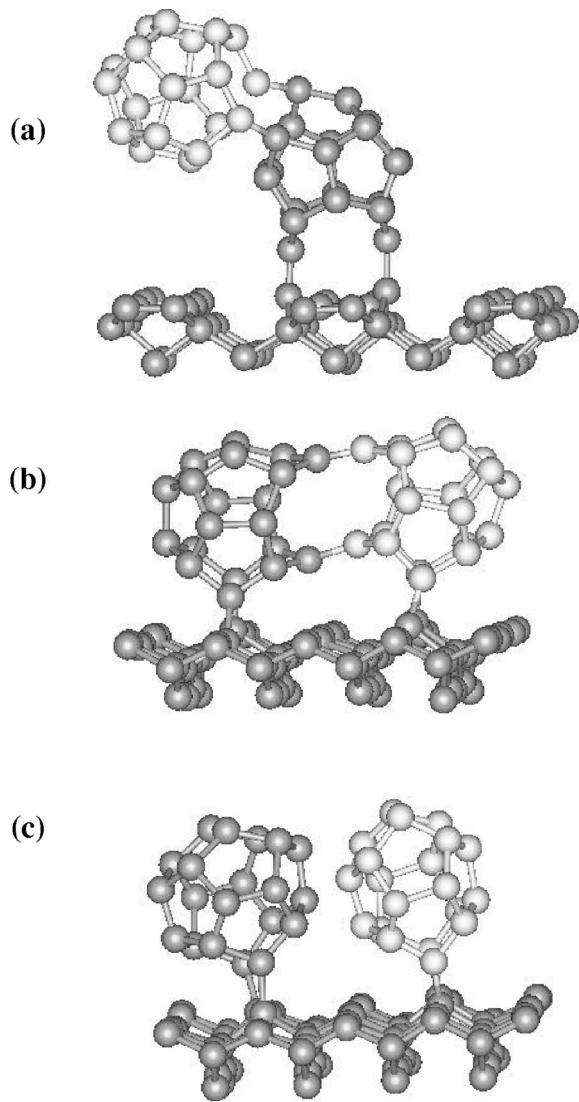


FIG. 4. Three typical chemisorption configurations (A, B, and C) observed by the deposition of cage II on surface A.

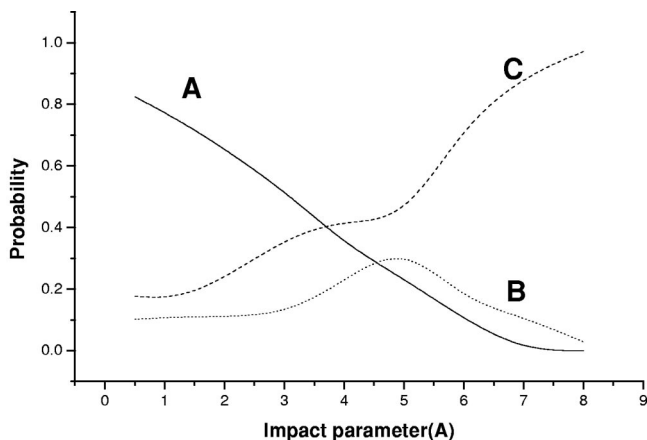


FIG. 5. The relative ratios corresponding to configurations A, B, and C presented in the deposition of cage II on surface A, which are dependent on the impact parameter  $p$ .

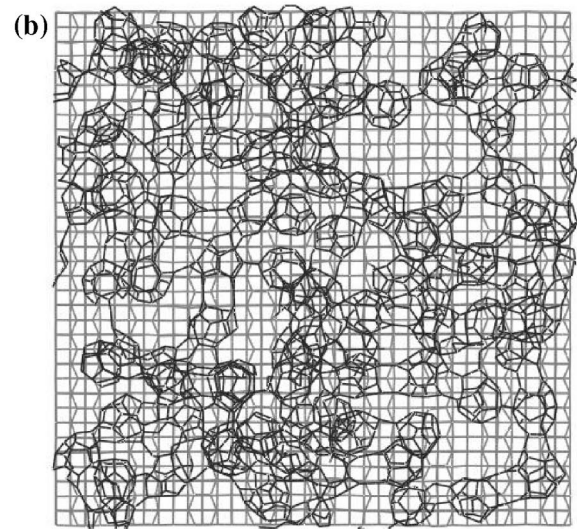
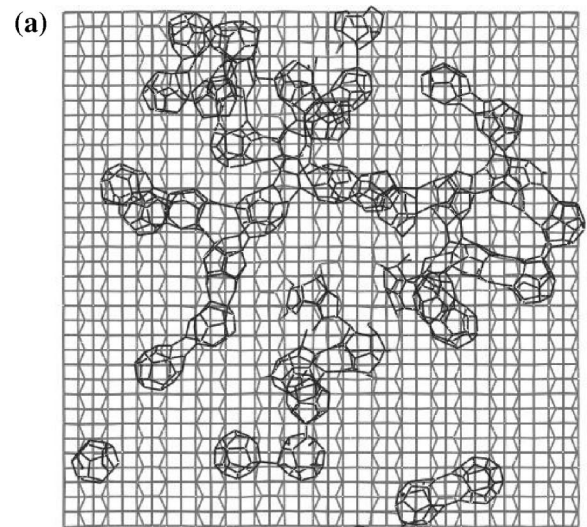


FIG. 6. Top view of atomic positions after (a) forty and (b) one hundred  $C_{20}$  fullerenes chemisorbed on the diamond surface, respectively.

tion, we deposited 147  $C_{20}$  fullerenes onto diamond surface, of which 100  $C_{20}$  fullerenes adsorbed on the surface and formed an adlayer. The top view of forty chemisorbed  $C_{20}$  fullerenes and one hundred chemisorbed  $C_{20}$  fullerenes on the diamond surface are presented in Figs. 6(a) and 6(b), respectively. As can be seen in the figures the adsorbed  $C_{20}$  clusters retain a cage structure similar to a slightly distorted free  $C_{20}$  fullerene. The local order in the adlayer in Fig. 6(b) was first analyzed quantitatively. The average neighbor-atom-number distribution of carbon atoms in the adlayer was calculated and is exhibited in Fig. 7(a). It was close to the distribution of free  $C_{20}$  cages except for the 15.2% of four neighbors. That was due to the bonds between cages. Furthermore, a peak at  $109^\circ$  was observed at the calculated bond angle distribution (see Fig. 8). The distribution of first neighbor distances in the film presents a peak at 0.147 nm with a full-width at half-maximum (FWHM) of 0.01 nm. Therefore, we conclude that the local-order of the film has a well de-

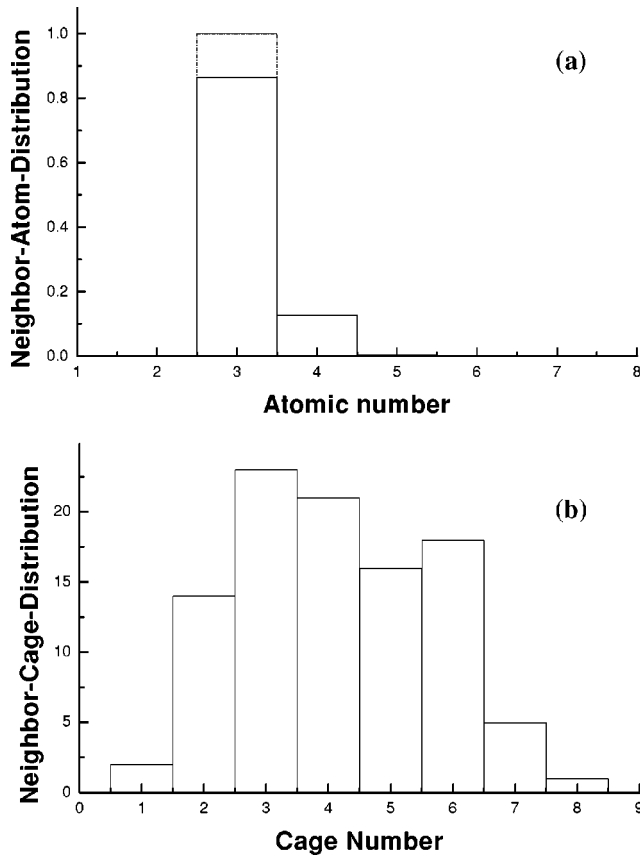


FIG. 7. (a) Comparison of the neighbor-atom-number distribution of atoms between one hundred chemisorbed  $C_{20}$  clusters and free clusters. The solid line represents the distribution of the chemisorbed clusters and the dashed line is for the free clusters. (b) The neighbor-cage-number distribution of the adsorbed  $C_{20}$  cages. The maximum neighbor cage-number even reaches 8.

finer  $sp^3$  character as that in the  $C_{20}$  fullerene. The strong correlation between the local order of the assembled diamondlike film and the incident free  $C_{20}$  clusters clearly demonstrates the memory effect proposed in LECBD experiments.

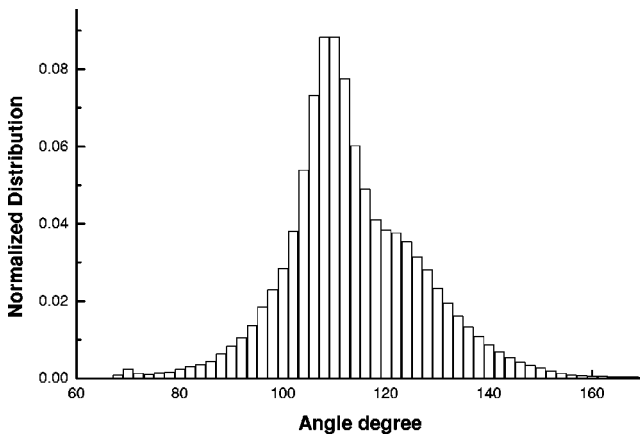


FIG. 8. The calculated bond angle distribution in the  $C_{20}$  cluster assembled film.

Finally the morphology of the  $C_{20}$  cluster-assembled film at the end of our simulation was studied in detail. As expected from the dangling bonds in the  $C_{20}$  cage, the adsorbed  $C_{20}$  could easily form bonds with each other, which is different from that of  $C_{60}$  and  $C_{28}$ .<sup>30</sup> At low coverage [Fig. 6(a)], the adlayer was composed of  $C_{20}$  dimers, trimers, and polymerlike chains. With increasing coverage, more bonds between  $C_{20}$  were formed. In Fig. 6(b), we observed that the sample was highly porous and all the adsorbed  $C_{20}$  cages were connected by C-C bonds. A giant molecule of  $C_{20}$  form was thus formed. This morphology was attributed to the strong  $C_{20}$ - $C_{20}$  interaction discussed in Sec. III B. The distribution of neighbor-cage number of the adsorbed  $C_{20}$  cages corresponding to the adlayer in Fig. 6(b) is shown in Fig. 7(b). On average, each  $C_{20}$  cage formed bonds with four cages and the maximum number of neighbor cages reached 8. This character was consistent with the higher reactivity of  $C_{20}$  as compared to the large fullerenes. The density of the assembled film was found to be  $1.34 \text{ g/cm}^3$ , which was much lower than that of diamond ( $3.42 \text{ g/cm}^3$ ) due to its porous structure. This calculated value was in reasonable agreement with experimental result ( $0.9 \text{ g/cm}^3$ ) (Refs. 1 and 12) if the size difference is taken (20–32) into account. Because the film formed by larger fullerenes may have lower density.<sup>31</sup>

In the growth process of  $C_{60}$  film, the film was able to undergo a disorder-to-order transition on the semiconducting surface due to the weak van der Waals interaction between  $C_{60}$  molecules.<sup>32</sup> But for  $C_{20}$  fullerene molecule, we did not observe any diffusion of the  $C_{20}$  cluster on the surface within the time scale of our simulation. This might be due to the strong covalent bonds between them which hampers rearrangement and diffusion. The deposited  $C_{20}$  film was heated after equilibrium to verify its thermal stability. During the heating process, we observed oscillations of polymerlike structures with no major structural change. The deposited film remained stable even at temperature up to 1500 K.

#### IV. CONCLUSION

The deposition of low-energy  $C_{20}$  fullerenes and the fabrication of  $C_{20}$  film on diamond (001)-(2×1) surfaces were simulated at atomic scale using the many-body Brenner potential. The focus of our investigation was on the film morphology, especially the local order. Moreover, the effect of competition between the cluster-cluster interaction and cluster-surface interaction on the film morphology was also studied. Our main results can be summarized as follows.

(1) The collision dynamics of  $C_{20}$  on a diamond surface is strongly dependent on its impact energy. Within the energy range 10–45 eV, the probability for chemisorption is high and the chemisorbed  $C_{20}$  retains its free cage structure. This energy range is consistent with the experimental values 10–20 eV, where the memory effect was proposed.<sup>12</sup>

(2) The  $C_{20}$  film grows as random compact cluster stacking just like that observed in experiments. It is highly porous and polymerlike structure due to the strong cluster-cluster interaction. Thus its density ( $1.34 \text{ g/cm}^3$ ) is much lower compared to that of the diamond. In addition, the deposited

film remains stable even at the temperature up to 1500 K.

(3) The local order of the  $C_{20}$  film assembled under the experimental energy range 10–20 eV, shows a well defined  $sp^3$  character as that in  $C_{20}$  fullerene. The strong correlation between the  $C_{20}$  cluster assembled film and the free  $C_{20}$  cage illustrates the memory effect observed in the LECBD experiment.

The  $C_{20}$  thin film thus assembled, is one kind of nanostructured diamondlike carbon film. It can be widely used in many fields such as machine tools and optical coatings due to its high hardness and wear resistance. Furthermore, the

film assembled with doped  $C_{20}$  cages is expected to be a promising candidate for superconductor with a high  $T_c$ ,<sup>11</sup> because the free cluster structure is preserved.

#### ACKNOWLEDGMENTS

This work was supported partly by the National Natural Science Foundation of China. One of authors, A.J.Du., would like to thank the support of the ZhongLu-Bohr Foundation and the innovation foundation of Fudan.

\*Email address: hoyk@fudan.ac.cn or zypan@fudan.ac.cn

<sup>1</sup>P. Melion *et al.*, Int. J. Mod. Phys. B **9**, 339 (1995).

<sup>2</sup>P. Milani and S. Iannotta, *Cluster Beam Synthesis of Nanostructured Materials* (Springer, Berlin, 1999).

<sup>3</sup>H.W. Kroto *et al.*, Nature (London) **318**, 162 (1985).

<sup>4</sup>*Science and Technology of Fullerene Materials*, edited by P. Bernier *et al.*, MRS Symposia Proceedings No. 359 (Material Research Society, Pittsburgh, 1995).

<sup>5</sup>A. Canning, G. Galli, and J. Kim, Phys. Rev. Lett. **78**, 4442 (1997).

<sup>6</sup>Barbara Goss Levi, Phys. Today **1**, 15 (2001).

<sup>7</sup>Horst Prinzbach *et al.*, Nature (London) **407**, 60 (2000).

<sup>8</sup>Mineo Saito and Yoshiyuki Miyamoto, Phys. Rev. Lett. **87**, 035503 (2001).

<sup>9</sup>Giulia Galli, Francois Gygi, and J. Christophe Golaz, Phys. Rev. B **57**, 1860 (1998).

<sup>10</sup>Adina K. Ott, Gregory A. Rechtsteiner, Christian Felix, Oliver Hampe, Martin F. Jarrold, and Richard P. Van Duyne, J. Chem. Phys. **109**, 9652 (1998).

<sup>11</sup>Yoshiyuki Miyamoto and Mineo Saito, Phys. Rev. B **63**, 161401 (2001).

<sup>12</sup>V. Paillard, P. Melinon, V. Dupuis, A. Perez, J.P. Perez, G. Guiraud, J. Fornazero, and G. Panczer, Phys. Rev. B **49**, 11 433 (1994).

<sup>13</sup>D.W. Brenner, Phys. Rev. B **42**, 9458 (1990).

<sup>14</sup>J. Tersoff, Phys. Rev. B **37**, 6991 (1988).

<sup>15</sup>D.W. Brenner, J.A. Harrison, C.T. White, and R.J. Colton, Thin Solid Films **206**, 220 (1991).

<sup>16</sup>R. Smith and K. Beardmore, Thin Solid Films **272**, 255 (1996).

<sup>17</sup>Y. Xia *et al.*, Phys. Rev. B **56**, 4979 (1997).

<sup>18</sup>A. Garg, J. Han, and Susan B. Sinnott, Phys. Rev. Lett. **81**, 2260 (1998).

<sup>19</sup>X.Z. Ke, Z.Y. Zhu, F.S. Zhang, F. Wang, and Z.X. Wang, Chem. Phys. Lett. **313**, 40 (1999).

<sup>20</sup>V. Parasuk and J. Almlot, Chem. Phys. Lett. **184**, 187 (1991).

<sup>21</sup>J.C. Grossman, Lubos Mitas, and Krishnan Raghavachari, Phys. Rev. Lett. **75**, 3870 (1995).

<sup>22</sup>A.J. Du *et al.*, Chem. Phys. Lett. **344**, 270 (2001).

<sup>23</sup>S. Nose, Mol. Phys. **52**, 255 (1984).

<sup>24</sup>W. Hoover, Phys. Rev. A **31**, 1695 (1985).

<sup>25</sup>L. Verlet, Phys. Rev. A **159**, 98 (1967).

<sup>26</sup>Z.Y. Man *et al.*, Eur. Phys. J. D **7**, 595 (1999).

<sup>27</sup>L. Vattuone, U. Valbusa, and M. Rocca, Phys. Rev. Lett. **82**, 4878 (1999).

<sup>28</sup>D.C. Jacobs, K.W. Kolasinski, S.F. Shane, and R.N. Zare, J. Chem. Phys. **91**, 3182 (1989).

<sup>29</sup>C.T. Reeves, J.D. Stiehl, C.B. Mullins, and G.O. Sitz, J. Vac. Sci. Technol. A **19**, 1543 (2001).

<sup>30</sup>W.J. Zhu *et al.*, J. Appl. Phys. **88**, 6836 (2000).

<sup>31</sup>D. Donadio, L. Colombo, P. Milani, and G. Benedek, Phys. Rev. Lett. **83**, 776 (1999).

<sup>32</sup>H. Xu, D.M. Chen, and W.N. Creager, Phys. Rev. Lett. **70**, 1850 (1993).